

Durham Research Online

Deposited in DRO:

20 October 2015

Version of attached file:

Accepted Version

Peer-review status of attached file:

Peer-reviewed

Citation for published item:

Nicholas, A.P. and Sambrook Smith, G.H. and Amsler, M.L. and Ashworth, P.J. and Best, J.L. and Hardy, R.J. and Lane, S.N. and Orfeo, O. and Parsons, D.R. and Reesink, A.J.H. and Sandbach, S.D. and Simpson, C.J. and Szupiany, R.N. (2016) 'The role of discharge variability in determining alluvial stratigraphy.', *Geology*, 44 (1). pp. 3-6.

Further information on publisher's website:

<http://dx.doi.org/10.1130/G37215.1>

Publisher's copyright statement:

Additional information:

Use policy

The full-text may be used and/or reproduced, and given to third parties in any format or medium, without prior permission or charge, for personal research or study, educational, or not-for-profit purposes provided that:

- a full bibliographic reference is made to the original source
- a [link](#) is made to the metadata record in DRO
- the full-text is not changed in any way

The full-text must not be sold in any format or medium without the formal permission of the copyright holders.

Please consult the [full DRO policy](#) for further details.

1 The role of discharge variability in determining alluvial
2 stratigraphy

3 **Andrew P. Nicholas¹, Gregory H. Sambrook Smith², Mario L. Amsler³, Philip J.**
4 **Ashworth⁴, James L. Best⁵, Richard J. Hardy⁶, Stuart N. Lane⁷, Oscar Orfeo⁸,**
5 **Daniel R. Parsons⁹, Arnold J.H. Reesink^{2,4,10}, Steven D. Sandbach^{1,6}, Christopher J.**
6 **Simpson⁴, and Ricardo N. Szupiany³**

7 *¹Geography, College of Life and Environmental Sciences, University of Exeter, Exeter,*
8 *EX4 4RJ, UK*

9 *²School of Geography, Earth and Environmental Sciences, University of Birmingham,*
10 *Birmingham, B15 2TT, UK*

11 *³Facultad de Ingeniería y Ciencias Hídricas, Centro Internacional de Estudios de*
12 *Grandes Ríos, Universidad Nacional del Litoral, C.C. 217 – (3000) Santa Fé, Argentina*

13 *⁴Division of Geography and Geology, School of Environment and Technology, University*
14 *of Brighton, Brighton, BN2 4GJ, UK*

15 *⁵Departments of Geology, Geography and Geographic Information Science, Mechanical*
16 *Science and Engineering and Ven Te Chow Hydrosystems Laboratory, University of*
17 *Illinois at Urbana-Champaign, Champaign, Illinois 61820, USA*

18 *⁶Department of Geography, Durham University, Durham, DH1 3LE, UK*

19 *⁷Faculté des géosciences et l'environnement, Institut de géographie, Université de*
20 *Lausanne, Batiment Anthropole, Lausanne, CH2015, Switzerland*

21 *⁸Centro de Ecología Aplicada del Litoral, Consejo Nacional de Investigaciones*
22 *Científicas y Técnicas, Corrientes, Argentina*

23 ⁹*Department of Geography, Environment and Earth Sciences, University of Hull, Hull,*
24 *HU6 7RX, UK*

25 ¹⁰*Geography and Environment, University of Southampton, Southampton, SO17 1BJ, UK*

26

27 **ABSTRACT**

28 We illustrate the potential for using physics-based modeling to link alluvial
29 stratigraphy to large river morphology and dynamics. Model simulations, validated using
30 Ground Penetrating Radar data from the Río Paraná, Argentina, demonstrate a strong
31 relationship between bar-scale set thickness and channel depth, which applies across a
32 wide range of river patterns and bar types. We show that hydrologic regime, indexed by
33 discharge variability and flood duration, exerts a first-order influence on
34 morphodynamics and hence bar set thickness, and that planform morphology alone may
35 be a misleading variable for interpreting deposits. Indeed, our results illustrate that rivers
36 evolving under contrasting hydrologic regimes may have very *similar morphology*, yet be
37 characterized by *marked differences* in stratigraphy. This realization represents an
38 important limitation on the application of established theory that links river topography to
39 alluvial deposits, and highlights the need to obtain field evidence of discharge variability
40 when developing paleoenvironmental reconstructions. Model simulations demonstrate the
41 potential for deriving such evidence using metrics of paleocurrent variance.

42

43 **INTRODUCTION**

44 Alluvial deposits are a key archive for reconstructing river morphology,
45 hydrology and paleoenvironments (Blum and Törnqvist, 2000; Miall, 2006). However,

46 interpretation of deposits is often difficult due to the lack of unambiguous criteria linking
47 fluvial processes to sedimentary product (Bridge, 2003; Ethridge, 2011), and because the
48 stratigraphic record is incomplete (Strauss and Sadler, 1989). Quantitative theory has
49 been used to relate bedform geometry and dynamics to bedset thickness (Paola and
50 Borgman, 1991). However, studies have necessarily focused on small spatial scales, such
51 as laboratory settings (Straub et al., 2012; van de Lageweg et al. 2013), or deposits
52 associated with individual bedform trains (Bridge and Best, 1997; Leclair, 2011).
53 Moreover, existing theory neglects the role of hydrologic variability (e.g., flood
54 magnitude and duration), despite its importance as a control on river evolution and
55 deposit reworking (Tamminga et al., 2015) and bar and bedform geometry (Wilbers et al.,
56 2003), all of which determine the resultant stratigraphy. Recent work highlights a need to
57 understand better the link between morphodynamics and sedimentology, particularly at
58 bar and channel belt scales, and for a range of river patterns and hydrologic regimes
59 (Fielding et al., 2009; Ethridge, 2011; Plink-Björklund, 2015). Achieving this aim has
60 proven virtually impossible to date due to a lack of suitable field data sets. However,
61 recent advances in numerical modeling mean that it is now possible to simulate river
62 morphodynamics over large temporal and spatial scales (Nicholas, 2013; Schuurman et
63 al., 2013). Herein, we aim to: (1) evaluate the potential for models to generate spatially-
64 rich data sets quantifying alluvial architecture; (2) elucidate the roles of hydrologic
65 regime and river pattern as controls on the resultant stratigraphy; and (3) identify some
66 key limitations on the application of existing theory linking alluvial deposits to their
67 formative flows.

68

69 **APPROACH**

70 The deposits of large sand-bed rivers were simulated using a physics-based
71 numerical model of hydraulics (for sub- and supercritical flows), sediment transport,
72 bank erosion and floodplain formation. This model, described and evaluated elsewhere
73 (Nicholas et al., 2013), is suitable for representing meandering, braided and anabranching
74 channels (Nicholas, 2013). Twenty-six simulations were conducted herein using a range
75 of bed slopes, sediment loads and bank erodibilities to generate rivers (50 km in length)
76 with contrasting channel patterns. All 26 simulations used the same hydrologic regime
77 (flood hydrographs where discharge varied from a low of $10,000 \text{ m}^3\text{s}^{-1}$ to a peak of up to
78 $30,000 \text{ m}^3\text{s}^{-1}$). In all simulations, the river evolved from a straight initial channel of
79 constant width. Simulation duration (typically 175 floods; nominally equivalent to a
80 scaled time period of 350 years) was sufficient to rework deposits multiple times. Herein,
81 we focus on six simulations that generated low-sinuosity anabranching channels similar
82 in form to the Río Paraná (Fig. 1), for which we have characterized the deposits of km-
83 scale bars using ground penetrating radar (GPR) and sediment cores up to 5 m in length
84 (Reesink et al., 2014). The Río Paraná has a mean annual discharge of $17,000 \text{ m}^3\text{s}^{-1}$ at
85 Corrientes, Argentina, where the geophysical surveys were based. To investigate the
86 influence of hydrologic regime on the stratigraphy, these six simulations were also run
87 with floods in which hydrograph duration was increased by factors of two and four, and
88 simulations that used a constant discharge of $22,500 \text{ m}^3\text{s}^{-1}$ (the average peak discharge for
89 simulated floods), yielding 44 simulations in total (see Table DR1 in the Data
90 Repository).

91 Modeled deposits were reconstructed from channel topography and flow
92 conditions at 700 points in time over the course of simulations. Bedsets, defined as
93 depositional elements bounded by erosional surfaces (Straub et al., 2012), were identified
94 from vertical profiles in each model grid cell (80 m by 40 m in size). Modeled sets are
95 associated with macro-scale morphologic features (e.g., unit bars) represented by the
96 model DEM, rather than smaller bedforms (e.g., dunes) that are finer than the model grid
97 resolution. Deposits were subdivided into three classes (termed ‘slackwater’, ‘ripples’
98 and ‘dunes’) based on modeled flow conditions. Slackwater deposits were classified as
99 those that form below a velocity threshold of 0.1 ms^{-1} , and the criterion of van Rijn
100 (1984) was used to define the ripple/dune transition (see his fig. 1). To account for the
101 existence of non-equilibrium dunes (e.g., on the falling limb of a flood), deposits were
102 only classified as ripples where the threshold for dune formation was not exceeded at any
103 point during the hydrograph. Simulations are characterized by zero net aggradation, and
104 hence total deposit thickness scales with maximum thalweg depth (typically 25–30 m).
105 Analysis of deposits is restricted to sediment below the vegetation that is established on
106 bar tops that are inundated infrequently.

107

108 **RESULTS**

109 Simulations that yield low-sinuosity anabranching rivers (e.g., Fig. 1A), similar in
110 form to the Río Paraná (Fig. 1B), are characterized by km-scale sand bars that grow by
111 vertical stacking of unit bars, and lateral accretion of bar wings that wrap around the bar
112 head. Modeled bar deposits (Fig. 1C) are composed of stacks of four to eight bar sets
113 (similar to the three to seven bar sets reported by Bridge and Lunt, 2006). Cross-bar

114 channel fills and slackwater sediments deposited in the lee of the bar are common in
115 simulations. Truncation of deposits by unit bar migration is common, as is reworking to
116 depths of 5–10 m below the bar surface (Fig. 1D). Comparison of model results with
117 GPR data from the Río Paraná (see Table DR2 in the Data Repository) indicates that the
118 model reproduces both the vertical dimensions of bar sets, and the tendency for sets to
119 thin toward the bar surface (Fig. 1E). Modeled deposits comprise 1%–3% slackwater
120 sediments (predominantly composed of silt) and 5%–30% ripples, compared to 30%
121 ripples and 3% silt/clay (deposited in slackwater areas) on average for bars from the Río
122 Paraná near Corrientes (Reesink et al., 2014).

123 Previous studies have applied existing theory (e.g., Paola and Borgman, 1991) to
124 relate set thickness to formative flow depth for large-scale strata generated by migrating
125 bars (Bridge and Lunt, 2006; van de Lageweg et al., 2013). Such analysis often involves
126 the assumption that the spatial distribution of bed topography at an instant in time is
127 representative of the temporal distribution of topography at a point in space (i.e., that
128 morphology is a reliable measure of morphodynamics). We demonstrate below that this
129 assumption may be unjustified. Despite this, we observe a strong positive relationship
130 between mean channel water depth, calculated as the average depth at all channel
131 locations and model time steps, and mean bar set thickness for all 26 simulations
132 conducted using the same variable hydrological regime (Fig. 2A). These simulations are
133 associated with a wide range of channel patterns and widths (total channel belt width
134 varies from 1.5 km to 7 km). We find no statistically significant difference in the ratio of
135 mean bar set thickness to mean flow depth between channels with low and high
136 width:depth ratios ($n = 13$ for both groups). Moreover, the transition from

137 wider/shallower (anabranching) to narrower/deeper (meandering) channels is associated
138 with a transition from unit bar dominated to scroll bar dominated deposits. These results
139 imply a near constant ratio of mean bar set thickness to mean flow depth irrespective of
140 bar type and channel pattern.

141 The six simulations with constant discharge plot well above the regression line in
142 Figure 2A, with bar set thickness for these simulations increasing by a factor of 1.6 on
143 average compared to equivalent simulations where discharge varies. This cannot be
144 explained fully by differences in morphology (e.g., channel width, depth or pattern).
145 Moreover, simulations run with constant and variable discharge experience similar
146 average rates of deposition and bed reworking over decadal timescales. Despite this, bar
147 set thickness exhibits a clear relationship with channel morphodynamics, as defined by
148 measuring the thickness (Δz) of packages of continuous erosion or deposition in all
149 individual model grid cells throughout simulations, in order to derive a probability
150 density function (pdf) of morphodynamic event magnitude (Fig. 2B). Simulations with
151 constant discharge experience an increase in both small ($|\Delta z| < 0.025$ m) and large ($|\Delta z| >$
152 2.25 m) scale erosion and deposition events, but a reduced frequency of intermediate
153 scale events, and an overall increase in the variance of vertical change increments. We
154 attribute this to two factors. First, bars aggrade until reaching the water surface, and
155 hence when discharge is constant, and water level changes are small, many bar surfaces
156 experience lower rates of vertical change. Second, cut and fill cycles driven by flood
157 hydrographs are absent under constant discharge, because temporal changes in flow
158 velocity (at any given location) are limited. This allows the duration and magnitude of
159 continuous deposition events to increase, thus promoting thicker sets. Similarly, where

160 flood hydrograph duration increases, periods of continuous deposition are also longer.
161 This promotes a positive relationship between flood duration and relative bar set
162 thickness (Fig. 2C). Significantly, the standard deviation of Δz values is an excellent
163 predictor of mean bar set thickness across all 44 simulations (Fig. 2D). Thus, while mean
164 bar set thickness is a function of mean channel depth, morphodynamics rather than
165 morphology is the dominant control on stratigraphy.

166 Further insight into these relationships can be derived by analysis of the
167 variability in paleocurrent directions associated with the deposits, defined by the modeled
168 velocity vectors at the time of sediment deposition, and by the ratio of the downstream
169 and cross-stream dimensions of facies units, defined as deposits characterized by similar
170 proportions of dunes, ripples or thick sets (see metrics used in Figure 3, Table 1, and
171 Table DR3 in the Data Repository). Simulations that use a variable discharge regime
172 (flood duration, $T = 2$ y) are characterized by distinct values of these metrics for both low
173 and high sinuosity channels. Moreover, low sinuosity anabranching channels generated
174 by variable and constant discharge regimes exhibit marked differences in deposit
175 characteristics, despite having similar morphology. Channels formed by constant
176 discharge exhibit lower variability in paleocurrent direction and facies units that are
177 preferentially elongated in the downstream direction. Vertical packages of each deposit
178 type (notably dunes) exhibit marked differences in thickness between contrasting channel
179 planforms (see Table 1). Moreover, where discharge is constant, sediment packages are
180 thicker on average compared to those generated under a variable discharge regime. This
181 is consistent with the inverse relationship between unit bar set thickness and discharge
182 variability suggested previously by Sambrook Smith et al. (2009), and indicates a

183 tendency for bar overtopping to be inhibited where discharge is constant. This limits the
184 occurrence of lateral bar-top flows and channels, and promotes flow streamlining that
185 encourages the elongation of deposits.

186

187 **SUMMARY**

188 This study illustrates the potential for using physics-based modeling to link river
189 morphodynamics to stratigraphy. Our results demonstrate that bar set thickness is a good
190 predictor of channel depth irrespective of river pattern, and associated differences in bar
191 type. However, depth estimates derived from bar set thickness data may be highly
192 sensitive to uncertainty in hydrologic regime. This suggests that paleoflow
193 reconstructions should attempt to assess the nature of discharge fluctuations, for instance
194 as expressed by reactivation surfaces that are not associated with bedform
195 superimposition.

196 Our simulations examine large rivers, such as the Rio Paraná, characterised by
197 low discharge variability ($Q_{var} = \text{annual range in discharge}/\text{mean discharge} < 2$) and
198 gentle slopes, that are dominated by sub-critical flows. Herein, we do not consider rivers
199 characterised by high discharge variability or flash floods (e.g., $Q_{var} > 100$; Fielding et
200 al., 2009), where deposits formed under supercritical flow may be abundant and
201 accretionary sets associated with bar migration may be poorly developed (Plink-
202 Bjorklund, 2015). Consequently, our conclusions regarding the significance of
203 hydrologic regime are almost certainly conservative.

204 Our results indicate that data quantifying paleocurrent variance and the
205 downstream and cross-stream dimensions of facies units may be valuable for constraining

206 hydrologic variability. However, such characteristics are also a function of channel
207 pattern, in particular sinuosity. These results also indicate that physical and numerical
208 models that impose a constant flow discharge may not be simulating correctly the alluvial
209 architecture of natural channels that experience discharge variability.

210 When relating bed topography to set thickness, some studies (e.g., van de
211 Lageweg, 2013) have assumed that the spatial distribution of bed heights (in bathymetric
212 data) is representative of the temporal distribution at a point in space. Our results
213 demonstrate that this need not be true. Modeled rivers with similar morphology can be
214 characterized by significant differences in temporal dynamics and hence stratigraphy.
215 Moreover, while a positive relationship between topographic variability and set thickness
216 is central to accepted theory (e.g., Paola and Borgman, 1991), we find that increased
217 hydrologic variability suppresses bar set thickness, due to its influence on
218 morphodynamics. Hydrologic regime thus plays a key role in controlling stratigraphy that
219 has yet to be incorporated within predictive theory. This implies that use of stratigraphic
220 evidence to link environment to morphology can only succeed by giving consideration to
221 the essential role of dynamics as a control on sediment accumulation and preservation.

222

223 **ACKNOWLEDGMENTS**

224 The authors are grateful to the UK NERC that funded this work (NE/E016022/1)
225 and the staff of CECOAL CONICET (Corrientes, Argentina) for their essential field
226 support. Simulations were performed using the University of Exeter Supercomputer. We
227 thank Chris Fielding, Piret Plink-Björklund, and Filip Schuurman for their thoughtful
228 reviews that helped us improve the manuscript.

229 **REFERENCES CITED**

- 230 Bridge, J.S., 2003, Rivers and Floodplains: Forms, Processes, and Sedimentary Record:
231 Oxford, UK, Blackwell Science Ltd, 504 p.
- 232 Bridge, J.S., and Best, J.L., 1997, Preservation of planar laminae due to migration of low
233 relief bed waves over aggrading upper stage plane beds: Comparison of experimental
234 data with theory: *Sedimentology*, v. 44, p. 253–262, doi:10.1111/j.1365-
235 3091.1997.tb01523.x.
- 236 Bridge, J.S., and Lunt, I.A., 2006, Depositional models of braided rivers: *International*
237 *Association of Sedimentologists Special Publication*, v. 36, p. 11–50.
- 238 Blum, M.D., and Törnqvist, T.E., 2000, Fluvial responses to climate and sea level
239 change: A review and look forward: *Sedimentology*, v. 47, p. 2–48,
240 doi:10.1046/j.1365-3091.2000.00008.x.
- 241 Ethridge, F.G., 2011, Interpretation of ancient fluvial channel deposits: Review and
242 recommendations: Tulsa, Oklahoma, Society for Sedimentary Geology (SEPM)
243 Special Publication, v. 97, p. 9–35.
- 244 Fielding, C.R., Allen, J.P., Alexander, J., and Gibling, M.R., 2009, Facies model for
245 fluvial systems in the seasonal tropics and subtropics: *Geology*, v. 37, p. 623–626,
246 doi:10.1130/G25727A.1.
- 247 Leclair, S.F., 2011, Interpreting fluvial hydromorphology from the rock record: Large-
248 river peak flows leave no clear signature: Tulsa, Oklahoma, Society for Sedimentary
249 Geology (SEPM) Special Publication 97, p. 113–123.
- 250

- 251 Miall, A.D., 2006, How do we identify big rivers? And how big is big?: *Sedimentary*
252 *Geology*, v. 186, p. 39–50, doi:10.1016/j.sedgeo.2005.10.001.
- 253 Nicholas, A.P., 2013, Morphodynamic diversity of the world's largest rivers: *Geology*,
254 v. 41, p. 475–478, doi:10.1130/G34016.1.
- 255 Nicholas, A.P., Ashworth, P.J., Sambrook Smith, G.H., and Sandbach, S.D., 2013,
256 Numerical simulation of bar and island morphodynamics in anabranching
257 megarivers: *Journal of Geophysical Research: Earth Surface*, v. 118, p. 2019–2044,
258 doi:10.1002/jgrf.20132.
- 259 Paola, C., and Borgman, L., 1991, Reconstructing random topography from preserved
260 stratification: *Sedimentology*, v. 38, p. 553–565, doi:10.1111/j.1365-
261 3091.1991.tb01008.x.
- 262 Plink-Björklund, P., 2015, Morphodynamics of rivers strongly affected by monsoon
263 precipitation: Review of depositional style and forcing factors: *Sedimentary*
264 *Geology*, v. 323, p. 110-147.
- 265 Reesink, A.J.H., et al., 2014, Scales and causes of heterogeneity in bars in a large multi-
266 channel river: Río Paraná, Argentina: *Sedimentology*, v. 61, p. 1055–1085,
267 doi:10.1111/sed.12092.
- 268 Sambrook Smith, G.H., Ashworth, P.J., Best, J.L., Lunt, I.A., Orfeo, O., and Parsons,
269 D.R., 2009, The sedimentology and alluvial architecture of a large braid bar, Río
270 Paraná, Argentina: *Journal of Sedimentary Research*, v. 79, p. 629–642,
271 doi:10.2110/jsr.2009.066.
- 272 Schuurman, F., Marra, W.A., and Kleinhans, M.G., 2013, Physics-based modeling of
273 large braided sand-bed rivers: Bar pattern formation, dynamics, and sensitivity:

- 274 Journal of Geophysical Research: Earth Surface, v. 118, p. 2509–2527,
275 doi:10.1002/2013JF002896.
- 276 Straub, K.M., Ganti, V., Paola, C., and Fofoula-Georgiou, E., 2012, Prevalence of
277 exponential bed thickness distributions in the stratigraphic record: Journal of
278 Geophysical Research: Earth Surface, v. 117, doi:10.1029/2011JF002034.
- 279 Strauss, D., and Sadler, P.M., 1989, Stochastic-models for the completeness of
280 stratigraphic sections: Mathematical Geology, v. 21, p. 37–59,
281 doi:10.1007/BF00897239.
- 282 Tamminga, A.D., Eaton, B.C., and Hugenholtz, C.H., 2015, UAS-based remote sensing
283 of fluvial change following an extreme flood event: Earth Surface Processes and
284 Landforms, v. 40, p. 1464–1476, doi:10.1002/esp.3728.
- 285 van de Lageweg, W.I., van Dijk, W.M., and Kleinans, M.G., 2013, Channel belt
286 architecture formed by a meandering river: Sedimentology, v. 60, p. 840–859,
287 doi:10.1111/j.1365-3091.2012.01365.x.
- 288 van Rijn, L.C., 1984, Sediment transport, Part III: Bedforms and alluvial roughness:
289 Journal of Hydraulic Engineering, v. 110, p. 1733–1754, doi:10.1061/(ASCE)0733-
290 9429(1984)110:12(1733).
- 291 Wilbers, A.W.E., and Ten Brinke, W.B.M., 2003, The response of subaqueous dunes to
292 floods in sand and gravel bed reaches of the Dutch Rhine: Sedimentology, v. 50,
293 p. 1013–1034, doi:10.1046/j.1365-3091.2003.00585.x.
- 294
295

296 Figure 1. (A) Simulated anabranching channel. Colour bars show water depth at low
297 flow, bed height above low flow and floodplain age; (B) Bar locations on the Río Paraná,
298 Argentina, at which GPR data shown in panel E were collected; (C) Modeled deposits
299 along the streamwise axis of a typical braid bar. Lines represent erosion surfaces (red),
300 morphological surfaces (black) and slackwater deposits (blue). Green bars indicate dunes.
301 Absence of green bar indicates ripples; (D) Time series of bed elevation at the location
302 within the grey box in panel (C); (E) Relationship between mean bar set thickness and
303 depth below bar surface for GPR data (circles) and simulations of low sinuosity
304 anabranching channels. Model results are shown at three points during each simulation,
305 for simulations with contrasting bank erodibility (E). Low values of E promote narrower,
306 deeper channels.

307

308 Figure 2. Plots of: A) Mean set thickness against flow depth; B) Probability density
309 functions of erosion and deposition event magnitude; C) Mean set thickness divided by
310 flow depth, shown for simulations that generate low sinuosity anabranching channels, run
311 with different hydrologic regimes (x axis) and contrasting bank erodibility (E); and D)
312 Mean set thickness vs the standard deviation of erosion and deposition events. In panels
313 A, C and D each point is a single simulation. Closed red squares are simulations that use
314 constant discharge; equivalent simulations with variable discharge are indicated by a
315 green triangle ($T = 2$ y where T is hydrograph duration), purple X ($T = 4$ y) and open
316 circle ($T = 8$ y); blue diamonds are all other simulations run with variable discharge ($T =$
317 2 y). Mean flow depth (in A and C) is the average for all channel locations and times.
318 Erosion and deposition magnitudes (Δz) in B and D are calculated as the total vertical

319 thickness of bed-level change within individual model grid cells during periods of
320 continuous erosion or deposition.

321

322 Figure 3. Deposit characteristics and channel morphology for rivers with contrasting
323 patterns and hydrologic regimes: (A) to (C) show the % of sediment in each grid cell
324 deposited in sets thicker than twice the mean set thickness for the river as a whole.
325 Results are shown for a meandering channel (A); low sinuosity anabranching channel
326 formed under variable discharge (B); and low sinuosity anabranching channel formed
327 under constant discharge (C). (D) to (F) show the standard deviation of the paleocurrent
328 direction (σ_V), for a braided river with sinuous individual channels (D); low sinuosity
329 anabranching channel formed under variable discharge (E); and low sinuosity
330 anabranching channel formed under constant discharge (F). (G) shows the morphology of
331 four typical simulated channels (from left to right: meandering, sinuous braided, low
332 sinuosity anabranching formed under variable discharge, and low sinuosity anabranching
333 formed under constant discharge). Color schemes in (G) are those used in Figure 1A.

334
335
336
337

338
339
340
341
342
343
344
345
346
347
348
349
350

351
 352
 353

TABLE 1. CHARACTERISTICS OF SIMULATED DEPOSITS

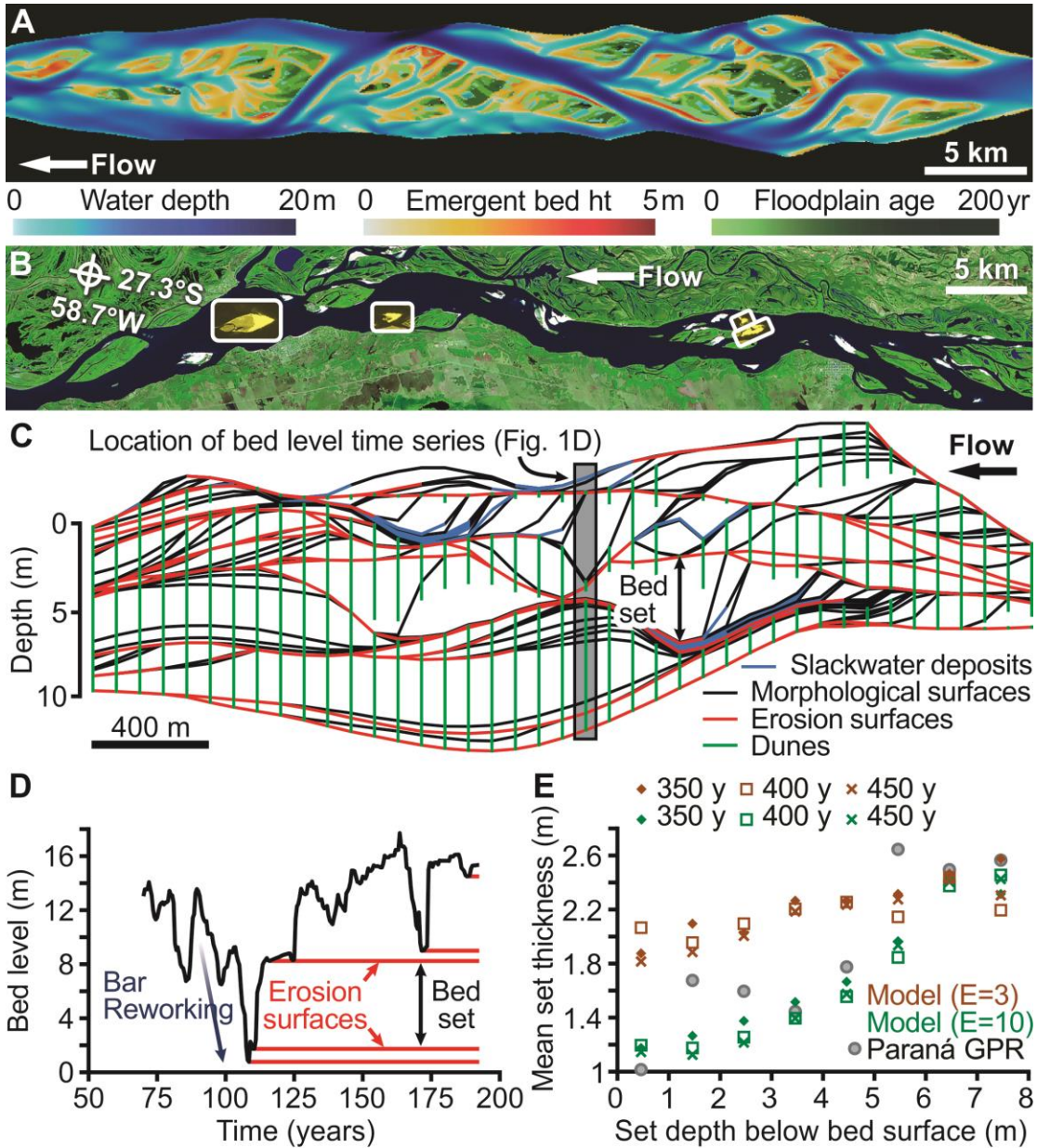
Channel pattern	Meandering	Sinuuous braided	Low-sinuosity anabranching	
	Variable (T = 2yr)	Variable (T = 2yr)	Variable (T = 2yr)	Constant
λ (m)	2.33	1.97	1.56	2.55
Lxy (Dune)	1.89	1.83	2.51	2.95
Lxy (Ripple)	2.01	1.91	2.71	3.22
Lxy (Large)	1.99	1.89	2.56	3.21
σ_{v90} (rad)	1.03	0.92	0.61	0.45
ψ (Dune)	7.54	3.80	2.26	5.37
ψ (Ripple)	0.44	0.66	0.75	1.69
ψ (Slackwater)	0.19	0.11	0.13	0.22

Note: Columns 2 and 3 show results for two simulations with contrasting morphology (see Fig. 3). Columns 4 and 5 show mean of results for six simulations of anabranching channels that use variable discharge (hydrograph duration, T = 2 yr) and constant discharge. λ is the mean set thickness. Lxy is the ratio of the average downstream and cross-stream lengths of contiguous model grid cells classified by deposit type as: Dunes (cells where >90% of sediment is classed as dunes); Ripples (cells where >10% of sediment is classed as ripples); and Large Sets (cells where >50% of sediment comprises sets thicker than twice the mean set thickness). σ_{v90} is the 90th percentile of the probability density function of the standard deviation of paleocurrent direction. ψ is the mean thickness of contiguous vertical packages of each deposit type.

354

355

356



357

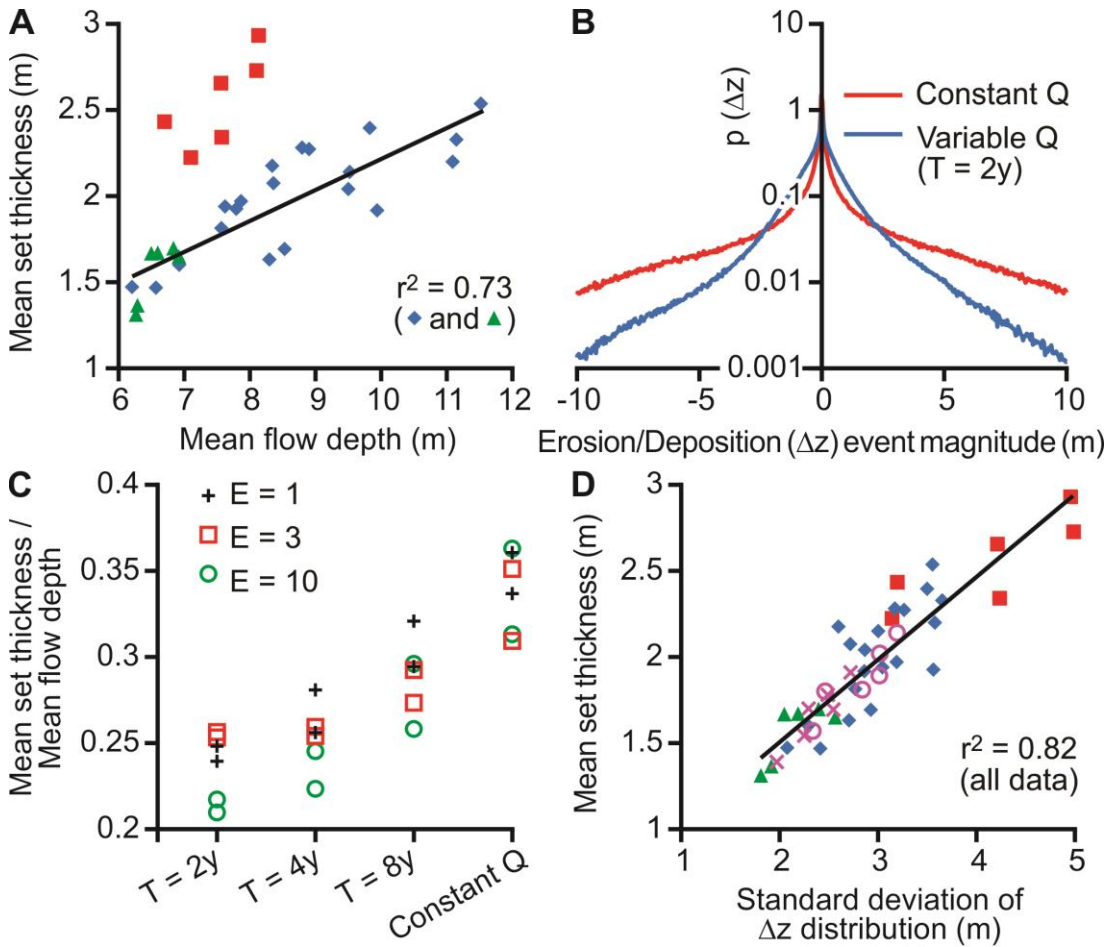
Nicholas et al. (Figure 1)

358

359

360

361



362

Nicholas et al. (Figure 2)

363

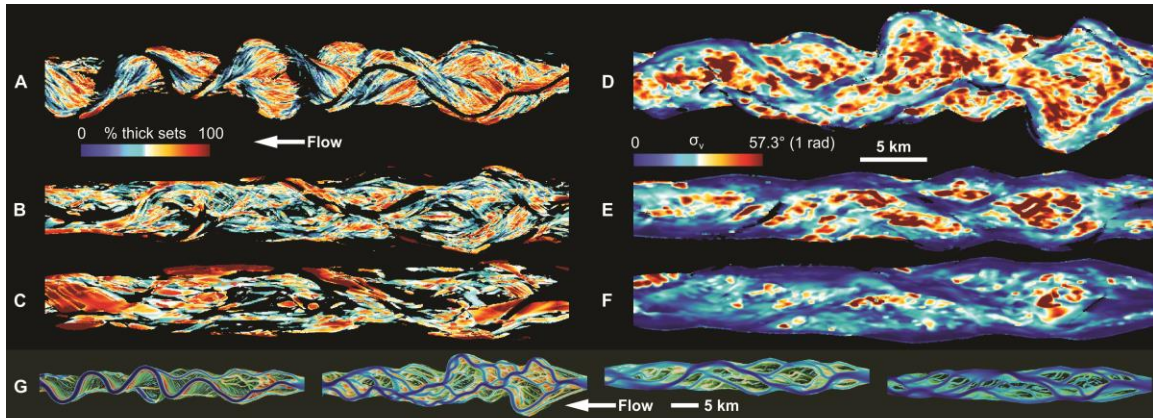
364

365

366

367

368



369

Nicholas et al. (Figure 3)